

Bloch Electrons in a Magnetic Field – Why Chaos Sends Electrons the Hard Way

R. Ketzmerick, K. Kruse, D. Springsguth, and T. Geisel

Max-Planck-Institut für Strömungsforschung und Institut für Nichtlineare Dynamik der Universität Göttingen,
Bunsenstr. 10, D-37073 Göttingen, Germany

We find that a two-dimensional periodic potential with different modulation amplitudes in x - and y -direction and a perpendicular magnetic field may lead to electron transport along the direction of *stronger* modulation and to localization in the direction of *weaker* modulation. This behaviour for Bloch electrons in a magnetic field is opposite to what one expects from the well studied Harper model, a one-band approximation. We demonstrate that the electron transport along the direction of stronger modulation is a quantum manifestation of non-integrability in the classical limit.

PACS numbers: 73.20.Dx, 05.45.+b, 73.50.Jt

The spectral properties of electrons in a spatially periodic potential, so-called Bloch electrons, and of electrons in a magnetic field were studied in the early days of quantum mechanics [1,2]: the periodic potential leads to Bloch bands, whereas Landau levels account for electrons in a magnetic field. For electrons subject to *both* [3,4], a two-dimensional periodic potential *and* a perpendicular magnetic field, there are two competing length scales, the period a of the potential and the magnetic length $l = \sqrt{\hbar/(eB)}$. If the ratio $a^2/(2\pi l^2)$, i.e., the number of magnetic flux quanta per unit cell is irrational, fascinating properties arise. The system has been studied mainly for the potential $V_x \cos(2\pi x/a) + V_y \cos(2\pi y/a)$ in a one-band approximation, the Harper model [5,6], which has the properties: i) For symmetric potentials, i.e., $V_x = V_y$, the spectrum (Hofstadter's butterfly) and eigenfunctions are multi-fractals [7–10] and thereby imply anomalous quantum diffusion [11,12]. ii) The quantized Hall conductance increases non-monotonically with Fermi energy obeying a diophantine equation [13]. iii) Upon changing the modulation amplitudes from $V_y > V_x$ to $V_y < V_x$ the Harper model shows a metal-insulator transition [14]. In the original two-dimensional model this transition corresponds to electron transport along the x -direction in the case $V_y > V_x$ and to transport along the y -direction in the case $V_y < V_x$ [4,15]. In the respective perpendicular direction wave packets are localized. Thus for $V_y \neq V_x$ transport occurs in the direction of *weaker* modulation only.

The one-band approximation, however, is appropriate only in the limiting cases where either the potential or the magnetic field can be treated as a weak perturbation [5,6]. This immediately raises the question whether the properties (i)-(iii) are mere artifacts of the one-band approximation. This question is not only of theoretical interest, but also of experimental relevance as current measurements [16,17] are performed in a regime where the one-band approximation is not adequate. Furthermore it is related to the question of the impact of classical non-integrability on quantum systems [18–20], as the one-band Harper model has an integrable classical limit,

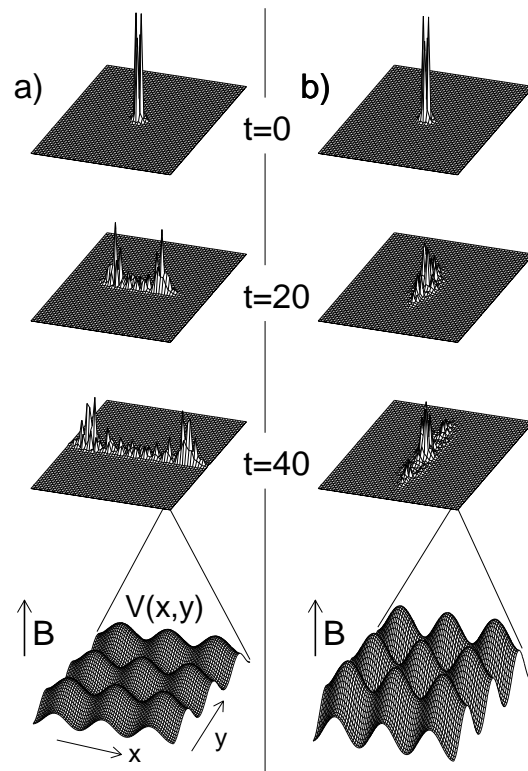


FIG. 1. Time evolution for initially localized electron wave packets spreading in two-dimensional periodic potentials with anisotropic modulation (bottom) and a perpendicular magnetic field. a) The wave packet spreads in the direction of *weaker* modulation only, as expected from a one-band approximation appropriate for potential strengths small compared to the magnetic field. b) In contrast for a larger potential strength with the same anisotropy the wave packet spreads in the direction of *stronger* modulation only. The time evolution is shown for a system size of 55×55 unit cells of the periodic potential and for times $t = 0, 20$ and 40 in units of the cyclotron period $2\pi/\omega_c$ with the wave packets energetically centered around $1.5 \hbar\omega_c$ corresponding to the second Landau level. The potential is given by Eq. (2) with $V_y/V_x = 1.25$, dimensionless potential strengths $K = 5$ (a) and $K = 10$ (b), and a magnetic field such that $\Phi/\Phi_0 = 89/55$. For the sake of visibility wave packet amplitudes for $t = 20$ and $t = 40$ are not drawn to scale.

whereas the original two-dimensional system of Bloch electrons in a magnetic field has a chaotic classical limit [21]. Studies of the influence of classical chaos on the energy spectrum (i) [22–24] and on the sequences of the quantized Hall conductance (ii) [25] show that both properties are changed only quantitatively, but not qualitatively compared to the Harper model and hence one might expect that the transport properties (iii) also remain qualitatively the same as in the Harper model.

In the present paper we demonstrate that this is not the case: We report a qualitatively new transport phenomenon, which is in striking contrast to the Harper model and demonstrates the limitations of this one-band description. For Bloch electrons in a magnetic field with different modulation amplitudes V_x , V_y we find that electron transport may occur along the direction of the *stronger* potential modulation while at the same time there is no transport in the perpendicular direction of weaker modulation [Fig. 1(b)]. We explain this transport phenomenon by studying the corresponding energy spectrum and eigenfunctions and by exploring the consequences of avoided band crossings reported recently [26]. Since for our system avoided band crossings are due to non-integrability in the classical limit, the peculiar transport in the direction of stronger modulation appears as a quantum signature of classical chaos. We argue that this feature of Bloch electrons in a magnetic field has observable consequences on transport measurements in semiconductor heterojunctions with lateral superlattices.

The one-particle Hamilton operator for an electron with charge $-e$ and effective mass m^* in a two-dimensional potential $V(x, y)$ has the form

$$H = \frac{1}{2m^*}(\mathbf{p} + e\mathbf{A})^2 + V(x, y), \quad (1)$$

where \mathbf{A} is the vector potential and the magnetic field $\mathbf{B} = \text{rot}\mathbf{A}$ is homogeneous and perpendicular to the xy -plane. The periodic potential

$$V(x, y) = V_x \cos(2\pi x/a) + V_y \cos(2\pi y/a), \quad (2)$$

has period a in both directions and we will concentrate on the case $V_y > V_x$. The properties of the system depend on the following three parameters [25]: the dimensionless potential strength

$$K = (V_x + V_y) 4\pi m^* a^2 / h^2, \quad (3)$$

the ratio V_y/V_x , and the ratio of the magnetic flux penetrating a unit cell of the potential divided by the magnetic flux quantum, i.e., $\Phi/\Phi_0 = a^2 B/(h/e)$. In this paper, we will vary only K , while $V_y/V_x = 1.25$ remains fixed and Φ/Φ_0 is a rational approximant of the golden mean $(\sqrt{5} - 1)/2$. We calculate eigenvalues and eigenfunctions using the approach described in Ref. [25] taking into account the four lowest Landau bands. From

the eigenvalues and eigenfunctions we then determine the time evolution of wave packets.

Figure 1 shows the time evolution of an initially localized wave packet [27] for two different values of K . For $K = 5$ one finds spreading in the x -direction and localization in the y -direction [Fig. 1(a)]. This agrees with what is known for the limit $K \ll 1$ [14,4,15] where the one-band approximation (the Harper model) is appropriate. In contrast, for $K = 10$ [Fig. 1(b)], surprisingly the wave packet spreads only in the direction of *stronger* modulation (y -direction), while it localizes in the direction of *weaker* modulation (x -direction). Thus with increasing potential strength the system shows a metal-insulator transition in the x -direction and simultaneously an insulator-metal transition in the y -direction. This change of the direction of transport cannot be explained on classical grounds as the corresponding classical system for the same parameters shows diffusion in the x - and y -direction.

In order to understand the origin of this phenomenon, we investigate the spectrum and eigenfunctions of the

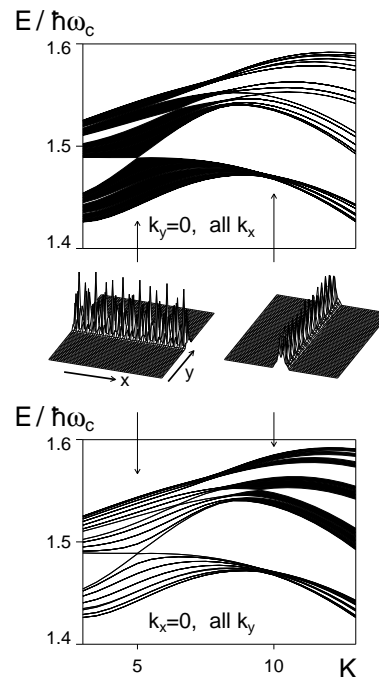


FIG. 2. The subspectra for wave numbers $k_y = 0$ and all k_x (top) and $k_x = 0$ and all k_y (bottom) as a function of the dimensionless potential strength K . They cover the energy range excited by the wave packets of Fig. 1 for the same system parameters. Increasing the value of K from 5 to 10 one finds a transition from bands to levels in the top subspectrum, while there is a dual transition from levels to bands in the bottom subspectrum. Consequently, the eigenfunctions [28] shown in the middle change from extended to localized in the x -direction and from localized to extended in the y -direction, explaining the time evolution found in Fig. 1.

operator (1). Numerically, this is feasible only for rational values of Φ/Φ_0 , but the properties of the system for an irrational value can be inferred by considering high rational approximants. For a rational number of magnetic flux quanta per unit cell $\Phi/\Phi_0 = q/p$ the operator (1) is periodic in the x - and y -direction with period pa and its eigenvalues consequently depend on the two wave numbers k_x and k_y in the magnetic Brillouin zone. Instead of considering the full spectrum of operator (1), i.e., the union of eigenvalues for all k_x and all k_y , we consider the subspectra built from the union of eigenvalues for fixed k_y (k_x) and all k_x (k_y). These subspectra contain information about the dynamics in the x -direction (y -direction) only, i.e., localized eigenfunctions give rise to narrow energy bands while broad bands are due to extended eigenfunctions. In Fig. 2 (top) the subspectrum for $k_y = 0$ and all k_x is shown as a function of the dimensionless potential strength K for the energy interval used for constructing the wave packets of Fig. 1. For $K = 5$, corresponding to the time evolution of Fig. 1(a), the spectrum consists of wide bands, indicating a metallic behavior in the x -direction, i.e., the direction of weaker modulation. In contrast, for $K = 10$, corresponding to Fig. 1(b), the spectrum consists of extremely narrow bands [28], indicating an insulating behavior in the x -direction. Figure 2 (bottom) shows the same spectral region, but now for the subspectrum for $k_x = 0$ and all k_y . As can be seen, the subspectra presented in Fig. 2 are dual to each other, i.e., whenever the spectrum consists of wide bands for fixed k_x it consists of narrow bands for fixed k_y and vice versa. This is also consistent with the directionality of typical eigenfunctions shown in Fig. 2 [29]. Thus, the change of direction of transport observed in Fig. 1 originates from changes in spectrum and eigenfunctions.

We will now explain the observed spectral properties and their changes. For $K = 0$ the operator (1) describes a free electron moving in a magnetic field. Therefore, the spectrum consists of infinitely degenerate Landau levels at $E/(\hbar\omega_c) = \nu + \frac{1}{2}$, where $\nu = 0, 1, 2, \dots$ and $\omega_c = eB/m^*$. For $K \neq 0$ the degeneracy is partially lifted. If K is small, each Landau level splits into a cluster of q bands which are p -fold degenerate (Fig 3). In this limit, these clusters are independent from each other and may be described in a one-band approximation by the Harper model [5,6]. For the case $V_y > V_x$, this approximation gives metallic behavior in x -direction and insulating behavior in y -direction for typical irrational values of Φ/Φ_0 [14], thus explaining the directional transport of Fig. 1(a) as well as spectrum and eigenfunctions of Fig. 2 for $K \leq 5$. But why does the direction of transport change to the perpendicular direction of stronger modulation when K is increased?

For larger values of K , the Harper model can no longer be used to describe the energy spectrum of the operator (1). Indeed, with increasing K the formerly well

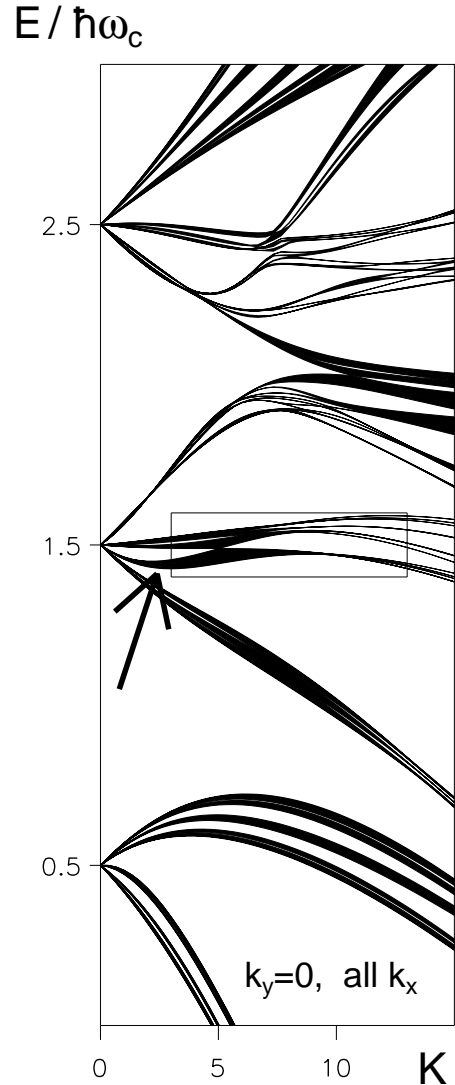


FIG. 3. The subspectrum for wave number $k_y = 0$ and all k_x as a function of the dimensionless potential strength K for the same parameters as in Fig. 1. Several avoided band crossings accompanied by transitions from energy *bands* to energy *levels* can be observed. The box indicates the region shown in Fig. 2 and the arrow points to the band that avoids crossing the central cluster of the second Landau band. In order to resolve individual levels in this figure we used $\Phi/\Phi_0 = 34/21$ instead of $\Phi/\Phi_0 = 89/55$, both being approximants of the golden mean.

separated clusters widen and approach each other. Since the corresponding classical limit is non-integrable one finds avoided crossings as a function of K (Fig. 3). It is just in regions of avoided crossings, where transitions from bands to levels occur. This phenomenon of metal-insulator transitions due to avoided band crossings was introduced in Ref. [26] in a very general context. Using perturbation theory it was shown how avoided crossings of spectra of one-band Hamiltonians change the effective

parameters of these Hamiltonians and how, in particular, this may lead to metal-insulator transitions. This general analysis of Ref. [26] applies just as well to Bloch electrons in a magnetic field and thus provides the final step for the explanation of the spectral changes observed in Figs. 3 and 2. It should be noted, though, that for such a complicated energy spectrum as in Fig. 3 the analysis of Ref. [26] cannot predict *where* these metal-insulator transitions occur. We would like to stress that the change of the direction of transport observed in Fig. 1 is a very general phenomenon for Bloch electrons in a magnetic field not restricted to the specific parameters chosen here.

Is it possible to observe this phenomenon experimentally? The obvious way to look for it would be in magnetotransport measurements for lateral superlattices on semiconductor heterojunctions similar to those of Refs. [16,17]: For small K , where the Harper model is appropriate, the system is metallic in the direction of weaker modulation and insulating in the perpendicular direction, independent of the Fermi energy. This should lead to a large ratio of ρ_{yy}/ρ_{xx} (for $V_y > V_x$). In contrast, for larger K the metallic and insulating direction change for Fermi energies where avoided band crossings have occurred, thus making ρ_{yy}/ρ_{xx} very small. In order to increase the likelihood of finding such changes, the experimental ratio of the modulation amplitudes V_y/V_x should be chosen not too far away from 1. Preliminary numerical studies indicate that the phenomenon is robust against weak disorder as present in the experimental probes.

In summary, for Bloch electrons in a magnetic field we have shown that classical non-integrability, leading to avoided band crossings and thereby to metal-insulator transitions, qualitatively changes the transport properties expected from the Harper model. In particular, chaos causes electron transport in the direction of stronger modulation.

ACKNOWLEDGMENTS

This work was supported in part by the Deutsche Forschungsgemeinschaft.

-
- [1] F. Bloch, Z. Phys. **52**, 555 (1929).
 [2] L. Landau, Z. Phys. **64**, 629 (1930).
 [3] R. Peierls, Z. Phys. **80**, 763 (1933); L. Onsager, Phil. Mag. **43**, 1006 (1952); J. Zak, Phys. Rev. **134**, A1602 (1964); E. Brown, Phys. Rev. **133**, A1038 (1964); D. Langbein, Phys. Rev. **180**, 633 (1969); G. M. Obermair und H.-J. Schellnhuber, Phys. Rev. B **23**, 5185 (1981).
 [4] For a review see, e.g., J. B. Sokoloff, Phys. Rep. **126**, 190 (1985).
 [5] P. G. Harper, Proc. R. Soc. London, Ser. A **68**, 874 (1955).
 [6] A. Rauh, Phys. Status Solidi B **69**, K9 (1975).
 [7] M. Ya. Azbel, Zh. Éksp. Teor. Fiz. **46**, 929 (1964) [Sov. Phys. JETP **19**, 634 (1964)].
 [8] D. R. Hofstadter, Phys. Rev. B **14**, 2239 (1976).
 [9] J. Bellissard und B. Simon, J. Funct. Anal. **48**, 408 (1982).
 [10] S. Ostlund and R. Pandit, Phys. Rev. B **29**, 1394 (1984).
 [11] H. Hiramoto and S. Abe, J. Phys. Soc. Jpn. **57**, 230 and 1365 (1988).
 [12] R. Ketzmerick, K. Kruse, S. Kraut, and T. Geisel, Phys. Rev. Lett. **79**, 1959 (1997).
 [13] D. J. Thouless, M. Kohmoto, M. P. Nightingale, and M. den Nijs, Phys. Rev. Lett. **49**, 405 (1982).
 [14] S. Aubry and G. André, Ann. Isr. Phys. Soc. **3**, 133 (1980).
 [15] A. Borelli, J. Bellissard, and F. Claro, to be published.
 [16] T. Schlösser, K. Ensslin, J. P. Kotthaus, und M. Holland, Europhys. Lett. **33**, 683 (1996).
 [17] C. Albrecht, J. H. Smet, D. Weiss, K. von Klitzing, V. Umansky, and H. Schweizer, Physica B **249-251**, 914 (1998).
 [18] M. C. Gutzwiller, *Chaos in classical and quantum mechanics* (Springer-Verlag, Berlin, Heidelberg, New York, 1991).
 [19] F. Haake, *Quantum signatures of chaos* (Springer-Verlag, Berlin, Heidelberg, New York, 1991).
 [20] *Quantum chaos: Between order and disorder*, published by G. Casati and B. V. Chirikov (Cambridge University Press, Cambridge, 1995).
 [21] T. Geisel, J. Wagenhuber, P. Niebauer, and G. Obermair, Phys. Rev. Lett. **64**, 1581 (1990); J. Wagenhuber, T. Geisel, P. Niebauer, and G. Obermair, Phys. Rev. B **45**, 4372 (1992).
 [22] G. Petschel and T. Geisel, Phys. Rev. Lett. **71**, 239 (1993).
 [23] O. Kühn, P. E. Selbmann, V. Fessatidis, H. L. Cui, and N. J. Horing, Phys. Rev. B **47**, 13019 (1993); O. Kühn, P. E. Selbmann, V. Fessatidis, and H. L. Cui, J. Phys., Condens. Matter **5**, 8225 (1993).
 [24] H. Silberbauer, P. Rotter, U. Rössler, and M. Suhrke, Europhys. Lett. **31**, 393 (1995).
 [25] D. Springsguth, R. Ketzmerick, and T. Geisel, Phys. Rev. B **56**, 2036 (1997).
 [26] R. Ketzmerick, K. Kruse, and T. Geisel, Phys. Rev. Lett. **80**, 137 (1998).
 [27] We construct the initial wave packet by taking $(x + iy) \exp[-(x^2 + y^2)/(4l^2)]$, an eigenfunction of the second Landau level for $K = 0$, and then by projecting it on the subspace of eigenfunctions for the given value of K with energies in the interval $[1.4 \hbar\omega_c, 1.6 \hbar\omega_c]$.
 [28] For rational approximants of an irrational Φ/Φ_0 the bands still have an exponentially small but finite width, which vanishes as Φ/Φ_0 is approached.
 [29] As the spectrum is p -fold degenerate, arbitrary linear superpositions of p linearly independent eigenfunctions for the same eigenvalue may look quite different. A given initial wave packet, however, singles out a certain linear superposition that determines its entire time evolution. The eigenfunctions shown in Fig. 2 are such linear superpositions determined by the initially localized wave packets of Fig. 1.